Nova Scientia
Revista de Investigación de la Universidad De La Salle Bajío

Revista Electrónica Nova Scientia

Análisis de la Cinética de Crecimiento de las Capas de Fe_2B Aplicadas durante Procesos de Borurización en un Acero AISI 1026
Diffusional Growth Kinetics Analisys of Fe_2B Layers Applied During the Coating Powder-Pack Boriding Process on an AISI 1026 Steel

M. Elias-Espinosa[1], J. Zuno-Silva[2], M. Ortiz-Domínguez[2], J. Hernández-Ávila[3] y O. Damián-Mejía[4]

[1] Instituto Tecnológico y de Estudios Superiores de Monterrey-ITESM Campus Santa Fe, D.F
[2] Ingeniería Mecánica, Universidad Autónoma del Estado de Hidalgo–Escuela Superior de Cd. Sahagún, Hidalgo
[3] Departamento de Materiales y Metalurgia, Universidad Autónoma del Estado de Hidalgo, Pachuca, Hidalgo
[4] Instituto de Investigación en Materiales, Universidad Nacional Autónoma de México-UNAM, D. F., México

México

Jorge Zuno Silva. E-mail: zunojorge@gmail.com

Resumen

La exigencia de emplear materiales con propiedades avanzadas incluyen la necesidad de aplicar recubrimientos de alta resistencia que alarguen la vida de útil de aceros comerciales, de esta forma, el tratamiento termoquímico de borurización tiene el potencial para cumplir estos requerimientos. En este trabajo de investigación se formula un modelo matemático para analizar la cinética de crecimiento de las capas de Fe_2B formadas sobre la superficie de un acero AISI 1026. El modelo matemático propuesto se desarrolló en base a la solución de la ecuación de balance de masa de la interface de crecimiento Fe_2B/Fe para evaluar el coeficiente de difusión del boro a través de las capas de Fe_2B en un rango de temperaturas de 1123 a1273 K. En el modelo desarrollado se incluyó el tiempo de incubación del boruro para formar la fase Fe_2B. El modelo matemático fue validado con datos experimentales realizados a una temperatura de 1253 K y tiempo de siete horas. Las capas de boruro fueron caracterizadas y analizadas por microscopia óptica y de barrido (se obtuvo un EDS), así como por Difracción de Rayos – X (XRD). Se utilizó la técnica de indentación Daimler-Benz Rockwell-C para evaluar cualitativamente la adherencia de la capa de Fe_2B sobre el sustrato (acero AISI 1026). Para usos prácticos y para un espesor determinado, se propuso un diagrama a espesor constante (215 μm) el cual es controlado con la variación de la temperatura y tiempo de exposición al recubrimiento. De los resultados obtenidos, se encontró que la energía de activación para el boro en el acero AISI 1026 es igual a 178 kJ mol^{-1}.

Palabras clave: bororizado, tiempo de incubación, modelo de difusión, cinética de crecimiento, energía de activación, adherencia

Recepción: 01-03-2014 *Aceptación: 09-02-2015*

Abstract

In the present study, a mathematical model was proposed for analyzing the growth of Fe_2B layers formed on AISI 1026 steel by the pack-boriding process. This model was based on solving the mass balance equations of the (Fe_2B/Fe) interface to evaluate the boron diffusion coefficients through the Fe_2B layers in the temperature range of 1123-1273 K. The boride incubation time for the Fe_2B phase was included in the present model. The suggested model was validated experimentally at a temperature of 1253 K for a treatment time of 7 h. Furthermore, the generated boride layers were analyzed by optical microscopy, scanning electron microscopy (SEM), energy dispersive spectroscopy (EDS) and X-ray diffraction analysis. The Daimler-Benz Rockwell-C indentation technique was used to qualitatively evaluate the adherence of the Fe_2B layer on the substrate. For practical use, an iso-thickness diagram was also proposed as a function of treatment time and temperature. The boron activation energy for AISI 1026 steel was found to be equal to 178.4 kJ mol^{-1} on the basis of our experimental results.

Keywords: boriding; incubation time; diffusion model; growth kinetics; activation energy; adherence

Nomenclature

α_{FeB} the thermal expansion coefficient of FeB layer (K^{-1}).

α_{Fe_2B} the thermal expansion coefficient of Fe_2B layer (K^{-1}).

v boride layer thickness (m).

k_{Fe_2B} is rate constant in the Fe_2B phase ($ms^{-1/2}$).

t_v is the effective growth time of the Fe_2B layer (s).

t is the treatment time (s).

$t_0^{Fe_2B}$ is the boride incubation time (s).

Q_{Fe_2B} the activation energy of the system ($Jmol^{-1}$).

$C_{up}^{Fe_2B}$ represents the upper limit of boron content in Fe_2B ($= 60\times10^3$ mol m^{-3}).

$C_{low}^{Fe_2B}$ is the lower limit of boron content in Fe_2B ($= 59.8\times10^3$ mol m^{-3}).

C_{ads}^{B} is the adsorbed boron concentration in the boride layer (mol m^{-3}).

$a_1 = C_{up}^{Fe_2B} - C_{low}^{Fe_2B}$ defines the homogeneity range of the Fe_2B layer (mol m^{-3}).

$a_2 = C_{low}^{Fe_2B} - C_0$ is the miscibility gap (mol m^{-3}).

C_0 is the terminal solubility of the interstitial solute (≈ 0 mol m^{-3}).

$C_{Fe_2B}[x(t)]$ is the boron concentration profile in the Fe_2B layer (mol m^{-3}).

$erf\left(x / 2\sqrt{D_{Fe_2B}t}\right)$ is the error function (it has no physical dimensions).

v_0 indicates the initial Fe_2B layer (m).

ε is the normalized growth parameter for the (Fe_2B/substrate) interface (it has no physical dimensions).

D_{Fe_2B} denotes the diffusion coefficient of boron in the Fe_2B phase (m^{2}s^{-1}).

$J_i[x(t)]$, (with $i = Fe_2B$ and Fe) are the fluxes of boron atoms in the (Fe_2B/substrate) inter face boundary (mol m^{-2}s^{-1}).

1. Introduction

Boriding is a well-known thermochemical treatment in which boron (because of its relatively small size) diffuses into the metal substrate to form hard borides. As a result of boriding, properties such as wear resistance, surface hardness and corrosion resistance are improved *(Sinha 1991, 437 -438).* Boriding can be carried with boron in different states such as solid powder, paste, liquid, gas and plasma. The most frequently used method is pack-boriding owing to its technical advantages *(Meric et al. 2000, 2168-2169).* Generally, the commercial boriding mixture is composed of boron carbide (B_4C) as donor, KBF_4 as an activator and silicon carbide (SiC) as a diluent to control the boriding potential of the medium. The boriding treatment requires temperatures ranging from 800 to 1000°C. Usually the treatment time varies between 0.5 and 12 h producing a boride layer of thickness depending on the boriding parameters (time and temperature). The morphology of the boride layer is affected by the presence of alloying elements in the matrix. Saw – tooth shaped layers are obtained in low –alloy steels or Armco iron whereas in high-alloy steels, the interfaces are smooth. According to the Fe-B phase diagram *(Okamoto 2004, 297),* two iron borides can be formed (FeB and Fe_2B).

A monophase Fe_2B layer with a tooth-shaped morphology is generally suitable for industrial application owing to difference between the specific volume and coefficient of thermal expansion of boride and the substrate *(Vipin 2002, 21-22)(Pertek 2002, 256-258).* The boron rich phase FeB is not preferred since FeB is more brittle and less tough than Fe_2B *(Vipin 2002, 21-22)(Pertek 2002, 256-258).* Furthermore, the brittleness of FeB layers causes a spalling when a high normal or tangential load is applied.

The modeling of the boriding kinetics is considered as a suitable tool to select the optimized parameters for obtaining a desired boride layer of the treated material for its practical use in industry. In particular, many models were reported in the literature for analyzing the growth of Fe_2B layers grown on different *substrates (Campos et al. 2003, 264-266) (Keddam et al. 2010, 5028-5029)* with and without the boride incubation times.

AISI 1026 steel is used on automotive industry to manufacture shaft and forged parts, but an improvemet on its wear properties is required. For this steel, a new diffusion model to stimate the borided layers is proposed with a just incubation time. Thus, on the current work, a diffusion model based on solving the masse balance equation at the (Fe_2B/ substrate) interface was

proposed to simulate the growth kinetics of Fe_2B layers grown on AISI 1026 steel. In the present model, the boride incubation time was taken independent on temperature. The pack-borided AISI 1026 was characterized by means of the following techniques: (optical microscopy, scanning electron microscopy, XRD and the Daimler-Benz Rockwell-C indentation technique). Based on experimental data, the boron activation energy was also evaluated when pack-boriding the AISI 1026 steel in the temperature range of 1123-1273 K.

2. Method

2.1 The kinetic model

The model takes into account the growth of Fe_2B layer on a saturated substrate with boron atoms as illustrated in **Figure 1.**

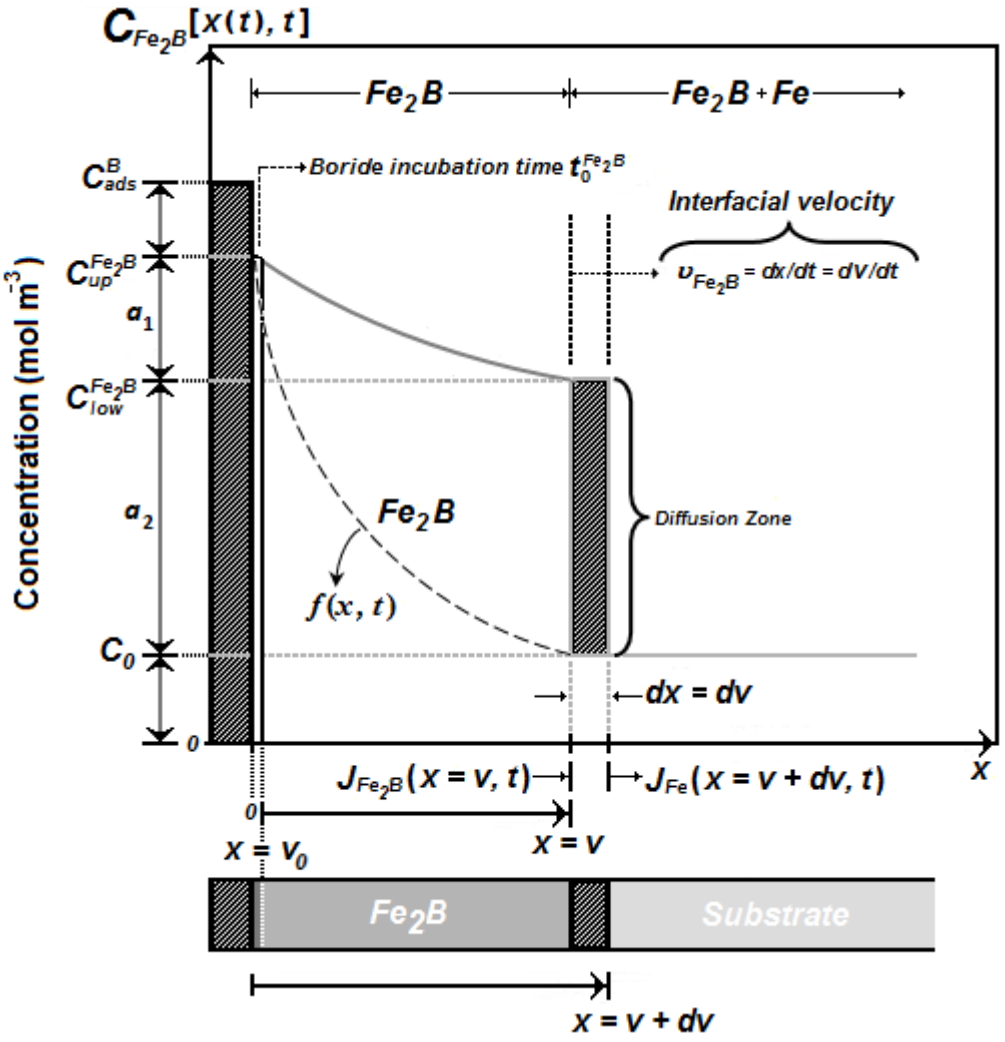

Figure 1. A schematic boron- concentration profile through the Fe_2B layer.

The $f(x)$ function represents the boron distribution in the ferritic matrix before the nucleation of Fe_2B phase. $t_0^{Fe_2B}$ corresponds to the incubation time required to form the Fe_2B phase when the matrix reaches a saturation state with boron atoms. $C_{up}^{Fe_2B}$ represents the upper limit of boron content in Fe_2B $(=60\times10^3\ \text{mol m}^{-3})$ *(Kulka et al. 2013, 197-199),* $C_{low}^{Fe_2B}$ is the lower limit of boron content in Fe_2B $(=59.8\times10^3\ \text{mol m}^3)$ and the point $x(t=t)=v$ represents the Fe_2B layer thickness, see **Figure 1**, *(Brakman et al. 1989, 1357-1359).*

The term C_{ads}^{B} is the effective adsorbed boron concentration during the boriding process *(Yu et al. 2005, 2364-2365).* From **Figure 1**, $a_1 = C_{up}^{Fe_2B} - C_{low}^{Fe_2B}$ defines the homogeneity range of the Fe_2B layer, $a_2 = C_{low}^{Fe_2B} - C_0$ is the miscibility gap and C_0 is the boron solubility in the matrix. This diffusion zone in the substrate underneath the compound layer can be ignored ($C_0 \approx 0$) *(Okamoto 2004, 297).* The following assumptions are considered for the diffusion model:

- The growth kinetics is controlled by the boron diffusion in the Fe_2B layer.
- The Fe_2B iron boride nucleates after a specific incubation time.
- The boride layer grows because of the boron diffusion perpendicular to the specimen surface.
- Boron concentrations remain constant in the boride layer during the treatment.
- The influence of the alloying elements on the growth kinetics of the layer is not taken into account.
- The boride layer is thin compared to the sample thickness.
- A uniform temperature is assumed throughout the sample.
- Planar morphology is assumed for the phase interface.

The initial and boundary conditions for the diffusion problem are represented as:

$$t = 0, x > 0, \text{ with: } C_{Fe_2B}[x(t), t = 0] = C_0 \approx 0. \quad (1)$$

Boundary conditions:

$$\left.\begin{array}{l} C_{Fe_2B}\left[x\left(t = t_0^{Fe_2B}\right) = v_0, t = t_0^{Fe_2B}\right] = C_{up}^{Fe_2B} \text{ (the upper boron concentration is kept constant),} \\ \text{for } C_{ads}^{B} > 60\times10^{3} \text{ mol m}^{-3}, \end{array}\right\} \quad (2)$$

$$\left.\begin{array}{l} C_{Fe_2B}[x(t = t) = v, t = t] = C_{low}^{Fe_2B} \quad \text{(the boron concentration at the interface is kept constant),} \\ C_{ads}^{B} < 59.8\times10^{3} \text{ mol m}^{-3}, \end{array}\right\} \quad (3)$$

v_0 is a thin layer with a thickness of ≈ 5 nm formed during the nucleation stage *(Dybkpv 2010, 7)*. Thus, $v_0 (\approx 0)$ when compared to the thickness of Fe_2B layer (v). The mass balance equation at the (Fe_2B/substrate) interface can be formulated by Equation (4) as follows:

$$\left(\frac{C_{up}^{Fe_2B} + C_{low}^{Fe_2B} - 2C_0}{2}\right)(A \cdot dv) = J_{Fe_2B}(x = v, t = t)(A \cdot dt) - J_{Fe}(x = v + dv, t = t)(A \cdot dt), \quad (4)$$

Where $A(=1\cdot1)$ is defined as the unit area and C_0 represents the boron concentration in the matrix. The flux J_{Fe_2B} and J_{Fe} are obtained from the Fick's First law as:

$$J_{Fe_2B}\left[x(t = t) = v, t = t\right] = -\left\{D_{Fe_2B}\partial C_{Fe_2B}\left[x(t = t) = v, t = t\right]/\partial x\right\}_{x = v}, \quad (5)$$

and

$$J_{Fe}\left[x(t = t) = v + dv, t = t\right] = -\left\{D_{Fe}\partial C_{Fe}\left[x(t = t) = v + dv, t = t\right]/\partial x\right\}_{x = v + dv} \quad (6)$$

The term J_{Fe} is null since the boron solubility in the matrix is very low (≈ 0 mol m^{-3}) *(Okamoto 2004, 297).*

Thus, Eq. (4) can be written as:

$$\left(\frac{C_{up}^{Fe_2B}+C_{low}^{Fe_2B}-2C_0}{2}\right)\frac{dx(t)}{dt}\bigg|_{x(t)=v}=-D_{Fe_2B}\frac{\partial C_{Fe_2B}[x(t=t),t=t]}{\partial x}\bigg|_{x(t)=v}. \quad (7)$$

If the boron concentration profile in Fe_2B is constant for the treatment time, Fick's Second law is reduced to an ordinary second-order differential equation as follows:

$$\frac{\partial C_{Fe_2B}[x(t),t]}{\partial t}=D_{Fe_2B}\frac{\partial^2 C_{Fe_2B}[x(t),t]}{\partial x^2}. \quad (8)$$

By solving Eq. (8), and applying the boundary conditions proposed in Eqs. (2) and (3), the boron concentration profile in Fe_2B is expressed by Eq. (9) if the boron diffusion coefficient in Fe_2B is constant for a particular temperature :

$$C_{Fe_2B}[x(t),t]=C_{up}^{Fe_2B}+\frac{C_{low}^{Fe_2B}-C_{up}^{Fe_2B}}{erf\left(\frac{v}{2\sqrt{D_{Fe_2B}t}}\right)}erf\left(\frac{x}{2\sqrt{D_{Fe_2B}t}}\right). \quad (9)$$

By substituting Eq. (9) into Eq. (7), equation (10) is obtained:

$$\left(\frac{C_{up}^{Fe_2B}+C_{low}^{Fe_2B}-2C_0}{2}\right)\frac{dv}{dt}=\sqrt{\frac{D_{Fe_2B}}{\pi t}}\frac{C_{up}^{Fe_2B}-C_{low}^{Fe_2B}}{erf\left(\frac{v}{2\sqrt{D_{Fe_2B}t}}\right)}\exp\left(-\frac{v^2}{4D_{Fe_2B}t}\right), \quad (10)$$

for $0 \le x \le v$.

Substituting the expression of the parabolic growth law: ($v=2\varepsilon D_{Fe_2B}^{1/2}t^{1/2}$) into Eq. (10), Eq. (11) is deduced:

$$\left(\frac{C_{up}^{Fe_2B}+C_{low}^{Fe_2B}-2C_0}{2}\right)\varepsilon=\sqrt{\frac{1}{\pi}}\frac{C_{up}^{Fe_2B}-C_{low}^{Fe_2B}}{erf\left(\varepsilon\right)}\exp\left(-\varepsilon^2\right). \quad (11)$$

The normalized growth parameter (ε) for the (Fe_2B/substrate) interface can be estimated numerically by the Newton-Raphson method. It is assumed that expressions $C_{up}^{Fe_2B}$, $C_{low}^{Fe_2B}$, and C_0, do not depend significantly on temperature (in the considered temperature range) *(Brakman et al. 1989, 1357-1359).*

A schematic representation of the square of the layer thickness against linear time ($v^2=4\varepsilon^2D_{Fe_2B}t=4\varepsilon^2D_{Fe_2B}\left(t_v+t_0^{Fe_2B}\right)$) is depicted in **Figure 2**. $t_v\left(=t-t_0^{Fe_2B}\right)$ is the effective growth time of the Fe_2B layer and t is the treatment time.

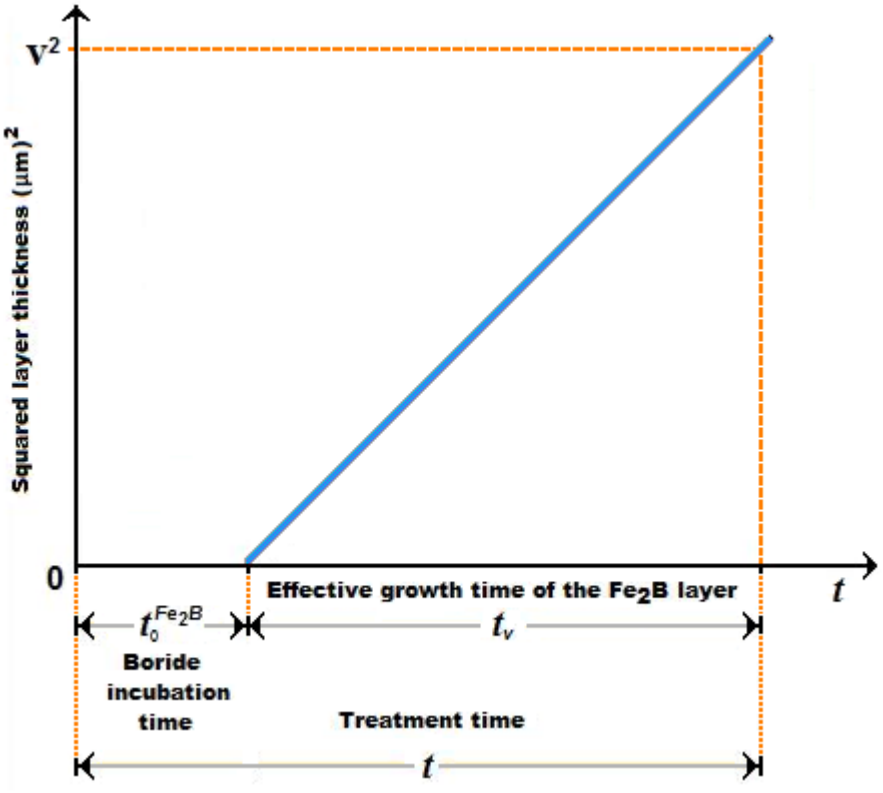

Figure 2. A Schematic representation of the square of the layer thickness against treatment time.

2.2. Experimental procedure

2.2.1. The boriding process

The material to be borided is AISI 1026 steel. It has a nominal chemical composition of 0.22-0.28 % C, 0.60-0.90% Mn, 0.07-0.6% Si, 0.050% S, and 0.040% P. The samples have a cubic shape with dimensions of 10 mm×10 mm×10 mm. Prior to the boriding process, the specimens were polished, ultrasonically cleaned in an alcohol solution and deionized water for 15 min at room temperature, and dried and stored under clean-room conditions.

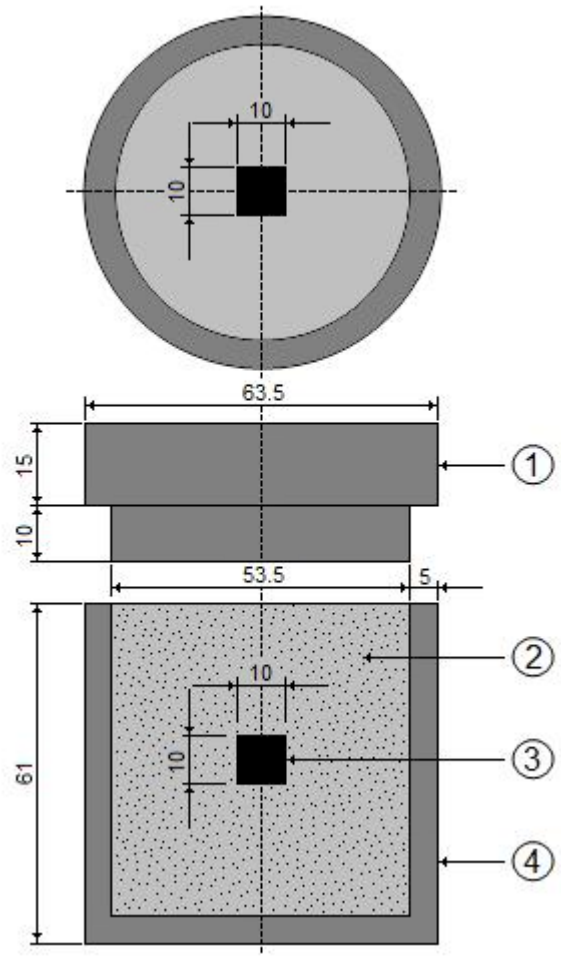

Figure 3. Schematic view of the stainless steel AISI 304L container for the pack-powder boriding treatment (1: lid; 2: powder boriding medium (B_4C + KBF_4 + SiC); 3: sample; 4: container).

The samples were packed along with a Durborid fresh powder mixture in a closed cylindrical case (AISI 304L) as shown in **Figure 3.** This powder mixture has an average size of 30 μm as illustrated on **Figure 4.**

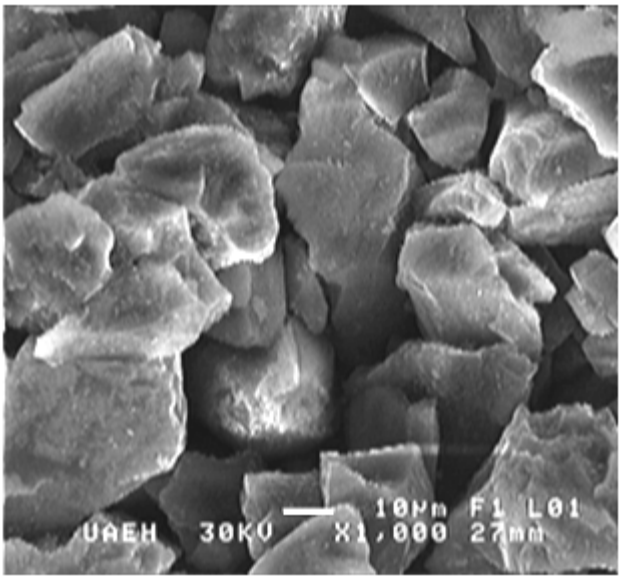

Figure 4. The powder boriding medium ($B_4C + KBF_4 + SiC$).

The powder-pack boriding process was carried out in a conventional furnace under a pure argon atmosphere in the temperature range of 1123 -1273 K. Four treatment times (2, 4, 6 and 8 h) were selected for each temperature. After the completion of boriding treatment, the container was removed from the furnace and slowly cooled to room temperature. As a result of preliminary experiments it was estimated that boriding started $t_0^{Fe_2B} \approx 31$ min approximately after transferring the specimen to the furnace; after that, the so-called boride incubation time sets in.

2.2.2. Microscopical observations of boride layers

The borided samples were cross-sectioned for metallographic examinations using a LECO VC-50 cutting precision machine. The cross-sectional morphology of the boride layers was observed with the Olympus GX51 optical microscope in a clear field. **Figure 5** shows the cress-sectional view of optical images of the Fe_2B layers of AISI 1026 steel formed at a temperature of 1173 K for different process durations. The resultant microstructure of Fe_2B layers appears to be very dense and homogenous, exhibiting a saw-toothed morphology. Since the growth of the saw-toothed boride layer is a controlled diffusion process with a highly anisotropic nature, higher temperatures and/or longer times encouraged the Fe_2B crystals to make contact with adjacent crystals and forced them to retain an acicular shape *(Palombarini – Carbucicchio 1987, 417).* It is seen that the thickness of Fe_2B layer increased with an increase of the boriding time (**Figure 5**)

since the boriding kinetics is influenced by the treatment time *(Campos-Silva et al. 2013, 415).* For a kinetic study, the boride layer thickness was automatically measured with the aid of MSQ PLUS software *(Ortíz-Dominguez, 2013).* To ensure the reproducibility of the measured layers thicknesses, fifty measurements were collected in different sections of the borided AISI 1026 steel samples to estimate the Fe_2B layer thickness; defined as an average value of the long boride teeth *(Campos-Silva 2010, 410).* All thickness measurements were taken from a fixed reference on the surface of the borided AISI 1026 steel, as illustrated in **Figure 6.**

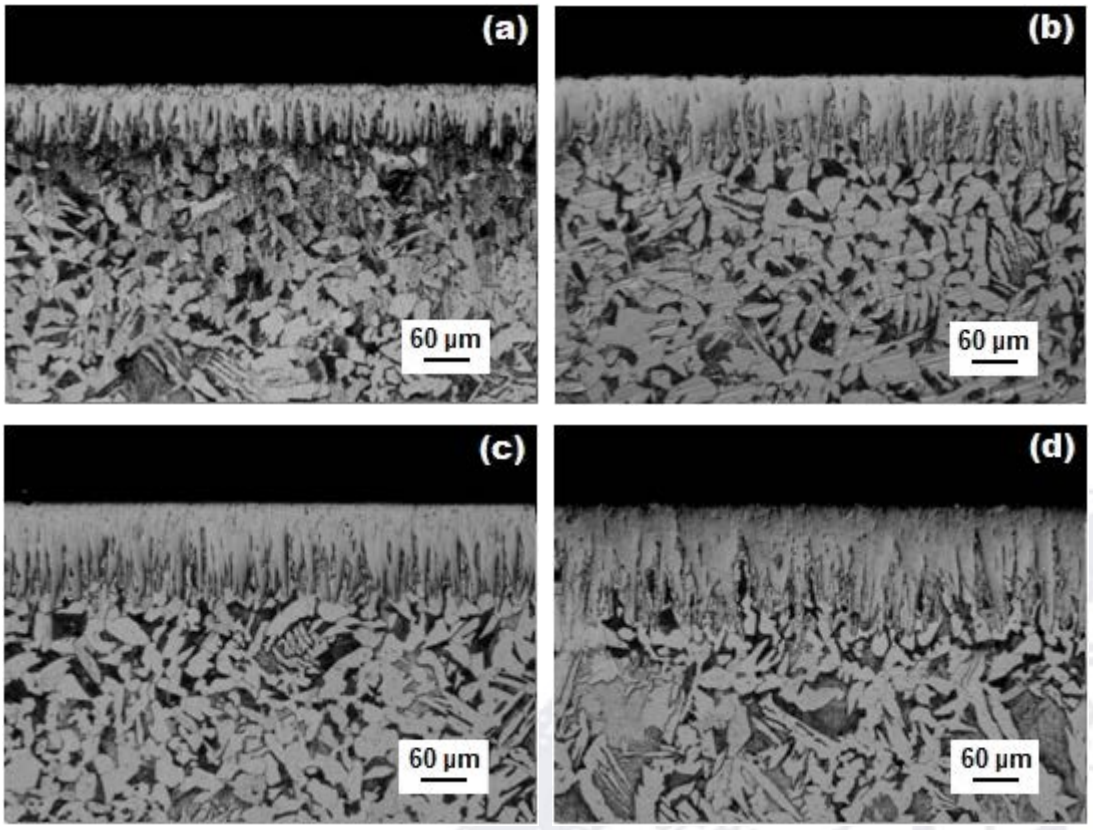

Figure 5. Optical micrographs of the boride layers formed at the surface of AISI 1026 steel treated at 1173 K during a variable time: (a) 2, 4, 6 and (b) 8 h.

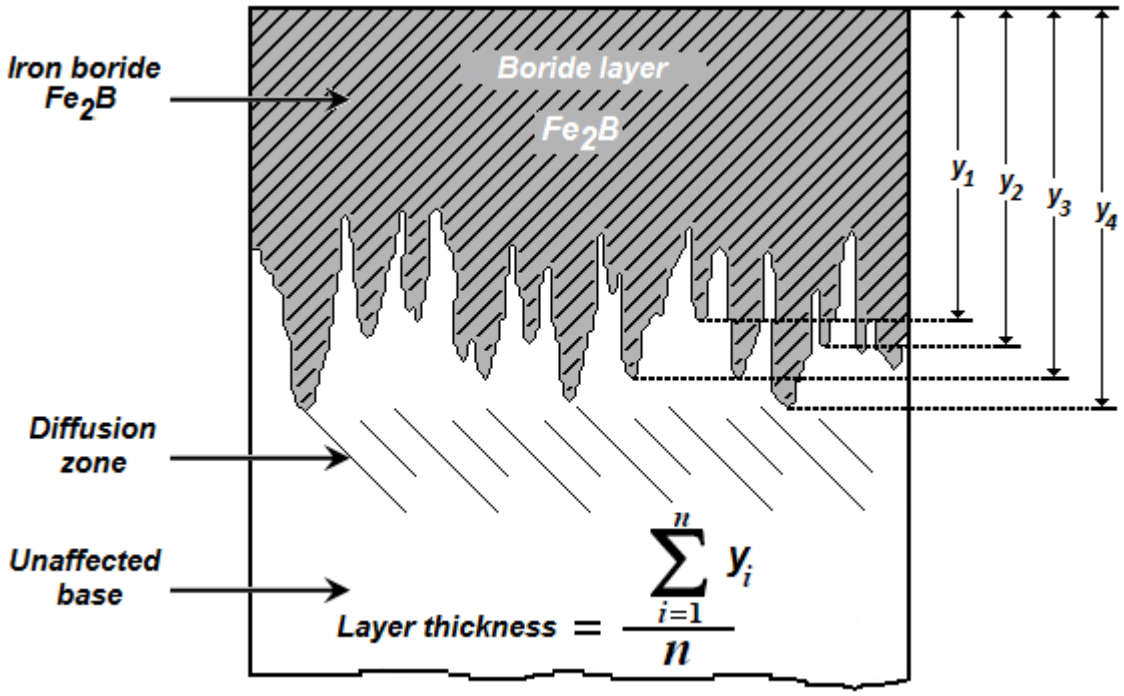

Figure 6. Schematic diagram illustrating the procedure for estimation of boride layer thickness in AISI 1026 steel.

The phases of the boride layers were investigated by an X-Ray Diffraction (XRD) equipment (Equinox 2000) using CoK_{α} radiation of 0.179 nm wavelength. The elemental distribution within the cross-section of boride layer was determined by Electron Dispersive Spectroscopy (EDS) equipment (JEOL JSM 6300 LV) from the surface. The Daimler-Benz Rocwell-C was performed to attain qualitative information on the adhesive strength of the boride layers to the substrate *(Verein, 1991, 4).* The well-known Rockwell-C indentation test is prescribed by the VDI 3198 norm, as a destructive quality test of coated compounds *(Vidakis et al. 2003, 483).* The principle of this method was reported in the reference work *(Taktak 2007, 1837 – 1839).* A load of 1471 N was applied to cause coating damage adjacent to the boundary of the indentation. Three indentations were conducted for each borided sample and scanning electron microscopy (SEM) was used to assess the adhesion test.

3. Results and discussions

3.1. SEM observations and EDS analysis

The cross- sectional view of SEM micrograph obtained on the borided AISI 1026 steel at 1223 K for 8 h, is shown in **Figure 7(a)**. The boride layer is grown on the substrate with a saw- toothed morphology. The needles of Fe_2B, with a difference in length, are visible on the SEM micrograph and penetrating into the substrate. This typical morphology is responsible of a good adhesion to the substrate. On this point, is important to know the behavior of the others alloy elements, as such Mn, Si, in the interphase and surface of the boride layer as explained ahead by an EDS analysis.

The cross section of SEM micrograph of the AISI 1026, borided at temperature of 1223 K for 8 h, is shown in **Fig. 7(a)**. The EDS analysis obtained by SEM is shown in **Fig. 7(b)** and **(c)**. The amounts of manganese appear to be lower than that of iron in the boride layer because of lower solubility. Thus, the deficiency of Mn results in a negative effect on the boride layer in terms of both thickness and morphology.

Fig. **7(c)** shows that the carbon and silicon do not dissolve significantly over the Fe_2B phase and they do not diffuse through the boride layer, being displaced to the diffusion zone, and forms together with boron, solid solutions like silicoborides ($FeSi_{0.4}B_{0.6}$ and Fe_5SiB_2) and boroncementite ($Fe_3B_{0.67}C_{0.33}$) [28].

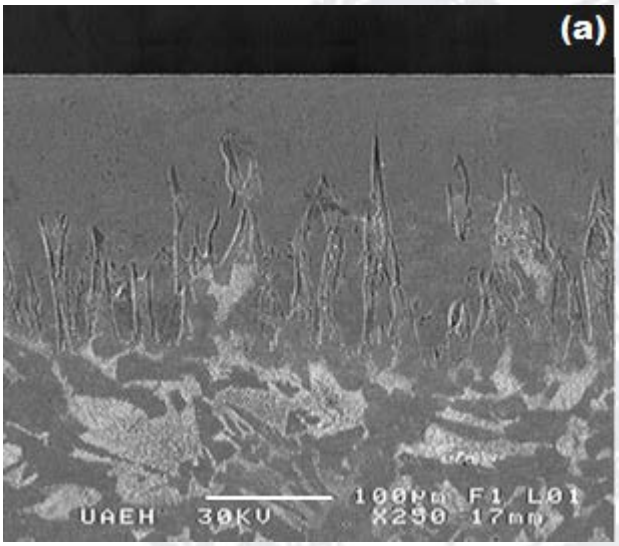

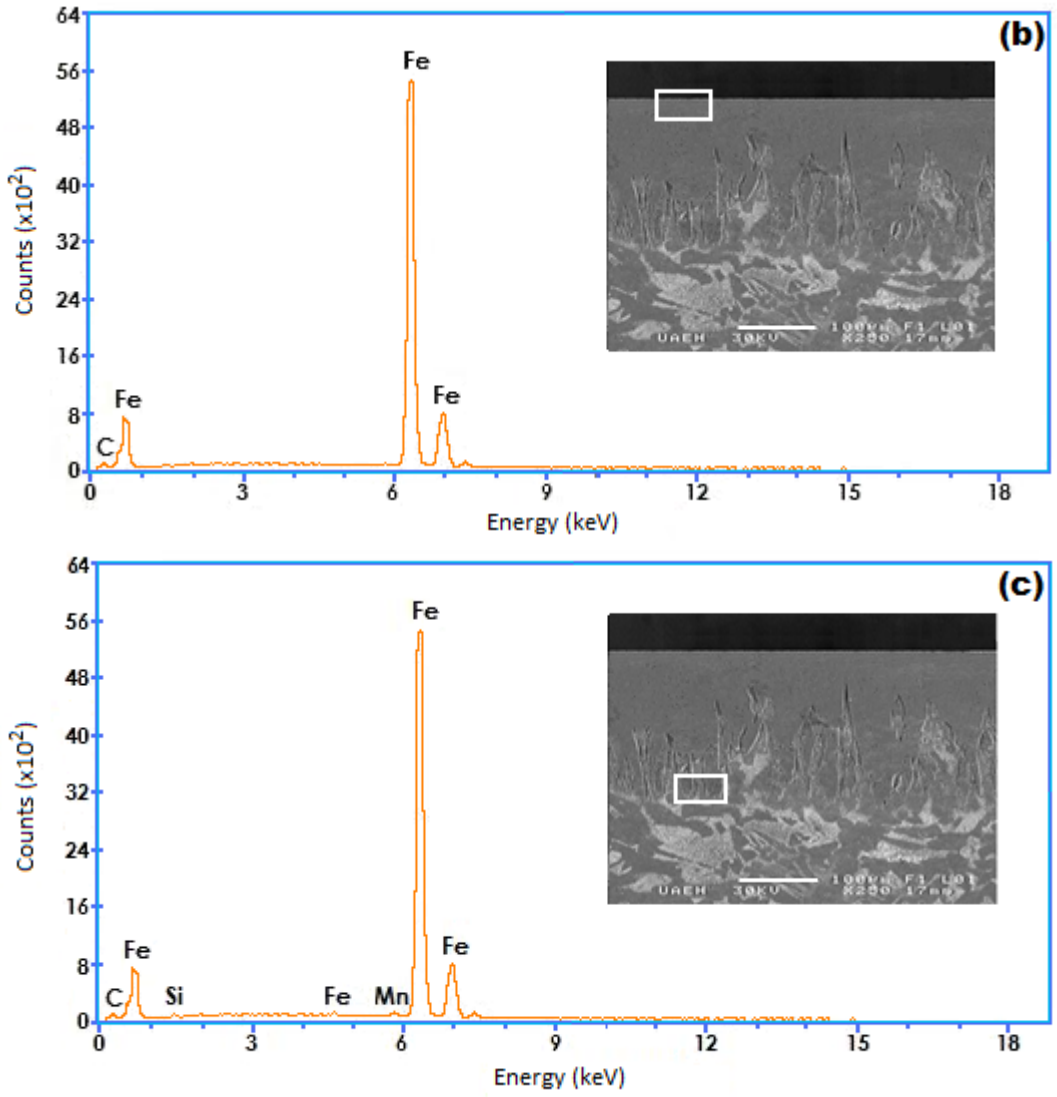

Figure 7. (a) SEM micrographs of the cross-sections of the borided AISI 1026 steel at 1223 K for 8 h, (b) EDS spectrum of borided sample at surface and (c) EDS spectrum of borided sample at interface.

3.2 X-ray diffraction analysis

Figure 8 shows the XRD pattern recorded on the surface of borided AISI 1026 steel at a temperature of 1273 K for a treatment time of 8 h. The diffraction peaks relative to the Fe_2B phase are easily identified.

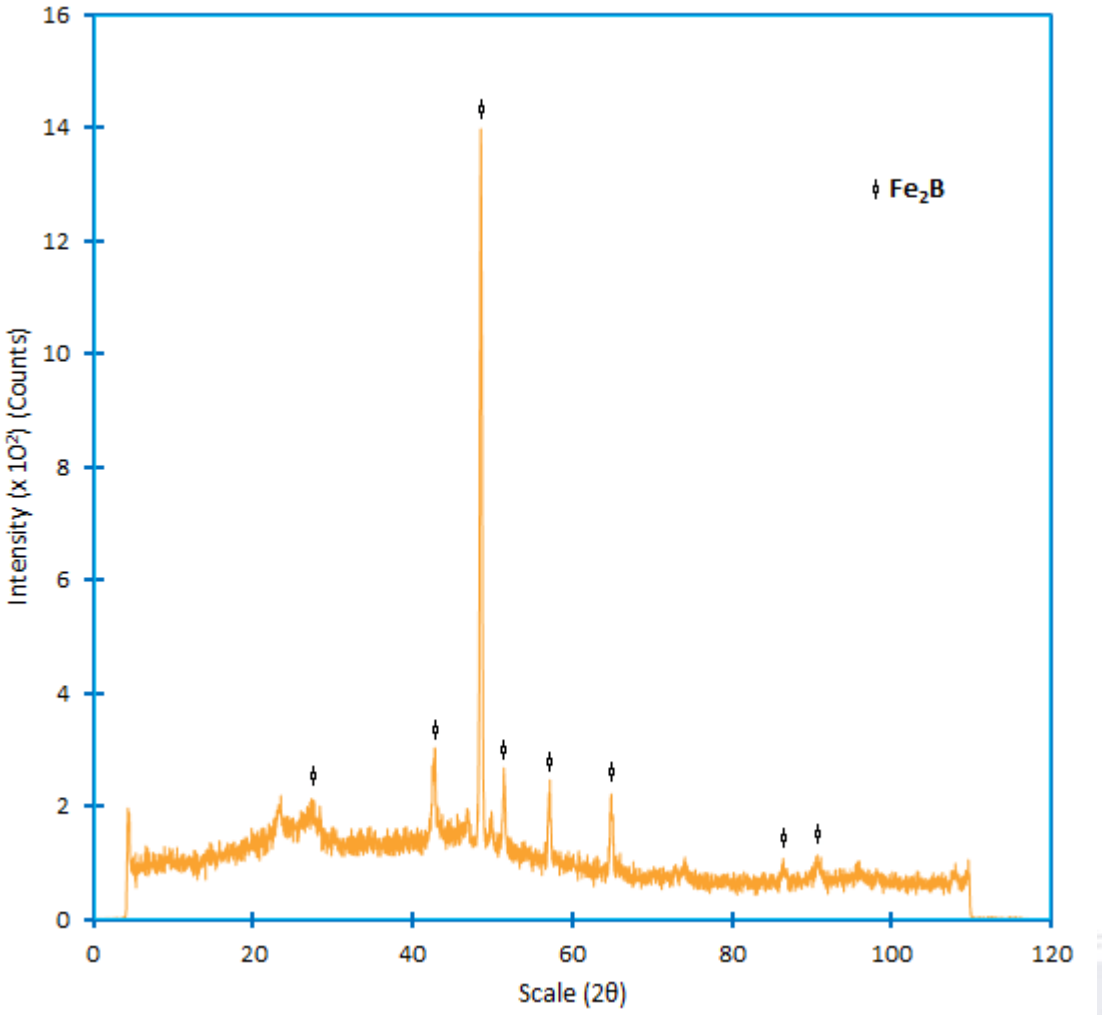

Figure 8. XRD pattern obtained at the surface of the borided AISI 1026 steel treated at 1273 K for 8 h, where the mains Fe_2B peaks are showed.

Crystals of the Fe_2B type orientate themselves with the z-axis perpendicular to the surface. Consequently, the peaks of the Fe_2B phase belonging to crystallographic planes, having a deviation from zero of the *l* index, showed increased intensities in the X-ray diffraction spectra *(Badini y Mazza 1988, 663-665).* The growth of boride layers is a controlled diffusion process with a highly anisotropic nature. In case of the Fe_2B phase, the crystallographic direction [001] is the easiest path for the boron diffusion in Fe_2B, because of the tendency of boride crystals to grow along a direction of minimum resistance, perpendicular to the external surface. As the metal surface is covered, an increasing number of Fe_2B crystals comes in contact with adjacent crystals and are forced to grow inside the metal, retaining an acicular shape *(Palombarini –*

Carbucicchio 1987, 415). In the powder-pack boriding, the active boron is supplied by the powder mixture. To form the Fe_2B phase on any borided steel, a low boron potential is required as reported in the reference works *(Vipin 2002, 21-22) (Bindal y Ucisik 1999, 209-211),* where a high amount of active boron in the powder mixture gives rise to the bilayer configuration consisting of FeB and Fe_2B.

3.3 Rockwell-C adhesion test

An indenter hardness tester was used to assess the Daimler-Benz Rockwell-C adhesion, as a destructive quality test for examined layers, it was employed for determination of cohesion. The well-know adhesion test prescribed by the VDI 3198 norm was used *(Verein, 1991, 4).* The principle of this method was presented in **Figure 9**. A conical diamond indenter penetrated into the surface of an investigated layer, thus inducing massive plastic deformation to the substrate and fracture of the boride layer.

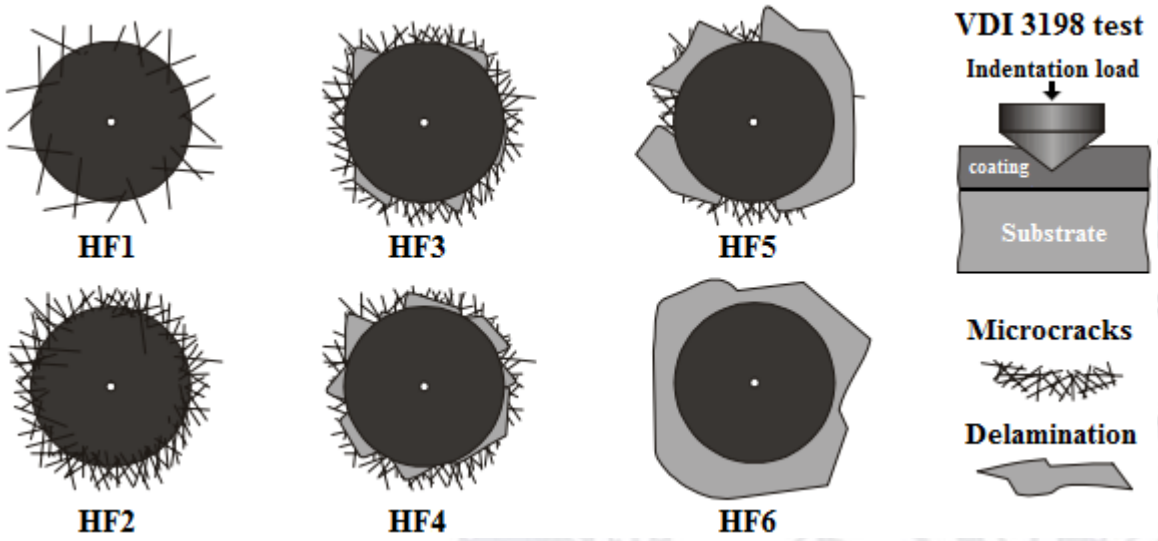

Figure 9. Principle of the VDI 3198 indentation test *(Verein, 1991, 4)*

The damage of the boride layer was compared with the adhesion strength quality maps HF1-HF6 (see **Figure 9**). ***In general, the adhesion strength HF1 to HF4 defined sufficient adhesion, whereas HF5 and HF6 represented insufficient adhesion (Verein, 1991, 4).*** Scanning Electron Microscope (SEM) images of the indentation craters for samples borided at 1273 K for 4 h are

given in **Figure 10**. The indentation craters obtained on the surface of the borided AISI 1026 revealed that there were radial cracks at the perimeter of indentation craters. However, a small quantity of spots with flaking of delamination was visible and the adhesion strength quality of this boride layer fits the HF3 category. In this context, the authors *S. Taktak and S. Tasgetiren (2006, 571-572)* have used the Daimler-Benz Rockwell-C adhesion technique to study the adhesion of boride layers grown on AISI H13 and AISI 304 steels. They found that their adhesion decreased with an increase of boriding time and temperature. *Rodriguez et al. (2009, 63)* also reported the adhesive strength of the boride layers using Daimler-Benz method.

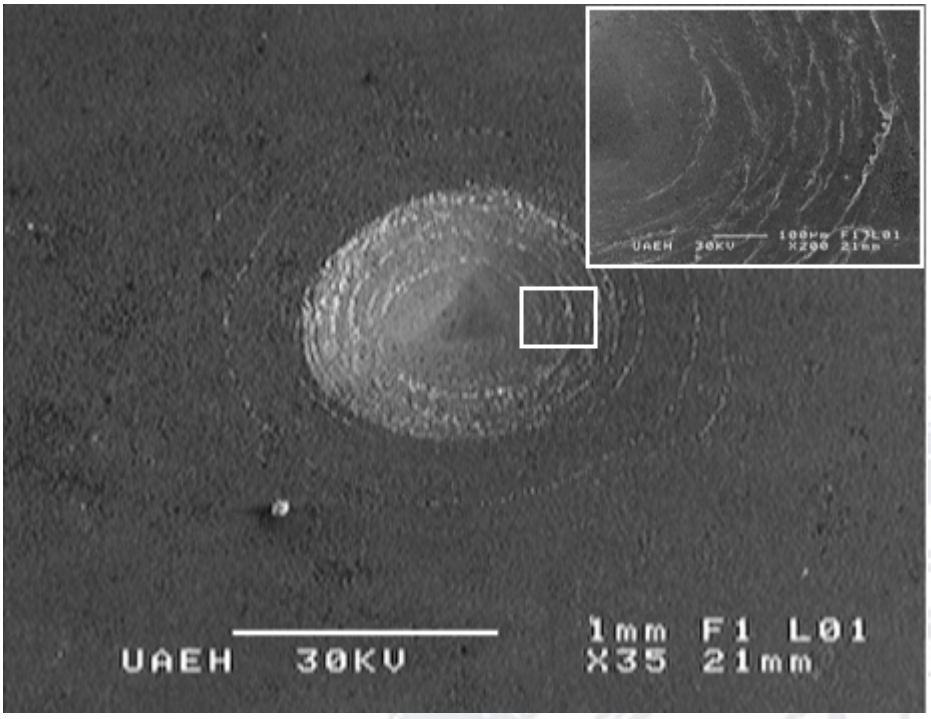

Figure 10. SEM micrograph showing the indentation of VDI adhesion test on AISI 1026.

3.4 Estimation of boron activation energy

The growth kinetics of Fe_2B layers formed on the AISI 1026 steel was used to estimate the boron diffusion coefficient through the Fe_2B layers by applying the suggested diffusion model. The determination of epsilon parameter (ε) is then required by solving the mass balance equation at the (Fe_2B/substrate) interface (see Eq. (11)) using the Newton-Raphson method. The

time dependence of the squared value of Fe_2B layer thickness is shown in **Figure 11**. The slopes of the straight lines in this figure provide the values of growth constants $(=4\varepsilon^2 D_{Fe_2B})$ for each boriding temperature. The value of boron diffusion coefficient in the Fe_2B layers can be determined by knowing the value of epsilon parameter. The boride incubation times for Fe_2B can also be deduced from the straight lines displayed in **Figure 11** by extrapolating to a null boride layer thickness.

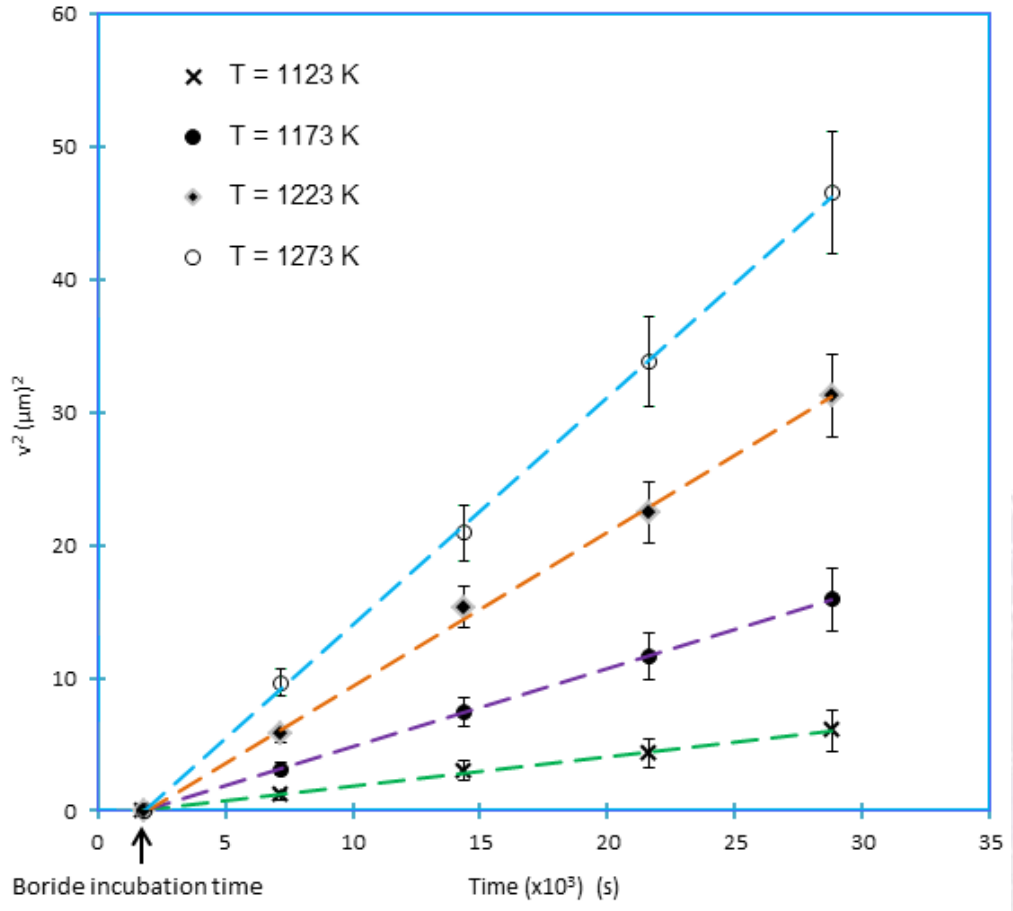

Figure 11. Averaged squares of the Fe_2B layers (v^2) vs. boriding time (t) at different temperature.

Table 1 summarizes the estimated value of boron diffusion coefficient in Fe_2B at each temperature along with the squared normalized value of epsilon determined from Eq. (11).

Table 1. The squared value of normalized growth parameter and boron diffusion coefficients in Fe_2B as a function of boriding temperature.

Temperatura (K)	Type of layer	ε^2 (Dimensionless)	$4\varepsilon^2 D_{Fe_2B}$ ($\mu m^2 s^{-1}$)
1123			$\mathbf{2.91\times10^{-1}}$
1173			$\mathbf{6.02\times10^{-1}}$
1223			$\mathbf{12.9\times10^{-1}}$
1273	**Fe_2B**	$\mathbf{1.747141\times10^{-3}}$	$\mathbf{20.9\times10^{-1}}$

To estimate the boron activation energy for the AISI 1026 steel, it is necessary to plot the natural logarithm of boron diffusion coefficient in Fe_2B versus the reciprocal temperature following the Arrhenius equation (see **Figure 12**). A linear fitting was adopted to obtain the temperature dependence of boron diffusion coefficient in Fe_2B with a correlation factor of 0.9782.

$$D_{Fe_2B} = 3.4\times10^{-3} exp\left(-178.4\ \text{kJmol}^{-1} / RT\right), \tag{12}$$

where: $R = 8.3144621$ [$\text{Jmol}^{-1}\text{K}^{-1}$] and T absolute temperature [K].

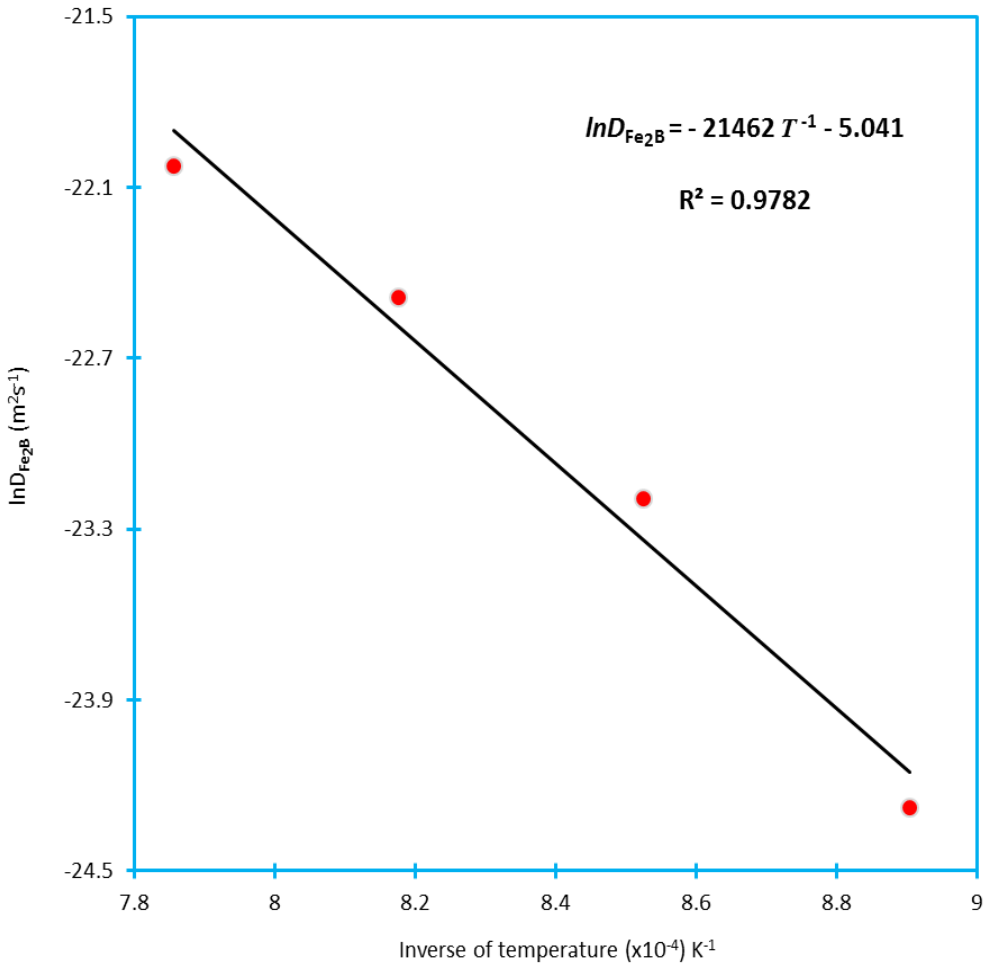

Figure 12. Boron diffusion coefficient (D_{Fe_2B}) as a function of boriding temperatures.

Table 2 shows a comparison of the boron activation energies in case of some borided steels *(Celik et al. 2008, 33-336) (Gunes et al. 2013, 569-570).* The found value of boron activation energy (= 178.4 kJ mol $^{-1}$) for AISI 1026 is slightly different from the reported value in (*Gunes et al. 2013, 569-570)* depending on the boriding conditions (using the liquid boriding method).

Table 2. A comparison of the boron activation energies for some borided steels.

Material	Boriding method	Boron activation energy (kJ mol $^{-1}$)	References
AISI 1020	Powder	110.3	[33]
AISI 1040	Powder	118.8	[33]
AISI 1018	Paste	153	[34]
AISI M2	Powder	207	[35]
AISI 316	Powder	198	[21]
AISI 8620	Plasma paste	99.7-108.8	[36]
AISI 8620 AISI 1026	Plasma paste Powder	124.7-138.5 178.4	[37] Present study

3.5 Validation of the diffusion model

The present model was validated by comparing the experimental value of Fe_2B layer thickness with the predicted result at a temperature of 1253 K for a treatment time of 7 h using Eq. (13):

$$v = 2\varepsilon D_{Fe_2B}^{1/2} t^{1/2} = \sqrt{17 D_{Fe_2B} t / 2500}\,. \tag{13}$$

In **Figure 13** is shown the optical image of the boride layer formed at 1253 K for 7 h of treatment.

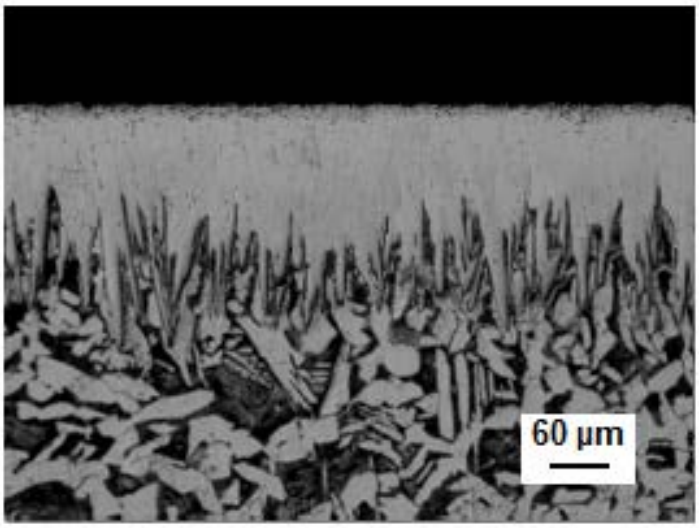

Figure 13. Optical micrographs of boride layer formed on AISI 1026 during powder-pack at the 1253 K of boriding temperature with an exposure time of 7 h.

Table 3 gives a comparison between the experimental value of Fe_2B layer thickness and the predicted one basis of Eq. (13). A good agreement was then obtained between the experimental value of Fe_2B layer thickness and the predicted one for the borided AISI 1026 steel at 1253 K for 7 h.

Table 3. Predicted and estimated values of the Fe_2B layer thickness obtained at 1253 K for a treatment time of 7 h.

Temperatura (K)	Type of layer	Boride layer thickness (µm) estimated by Eq. (13)	Experimental boride layer thickness (µm)
1253	Fe_2B	200.86	189.84 ± 11.29

3.5 Future exploitation of the simulation results

This kinetic approach can be used as a tool to determine the Fe_2B layer thickness as a function of boriding parameters (time and temperature) for AISI 1026 steel. Eq. (13) predicts the Fe_2B layer thickness for any temperature and boriding time. An iso-diagram thickness was plotted as a function of the temperature and exposure time as shown in **Figure 14**.

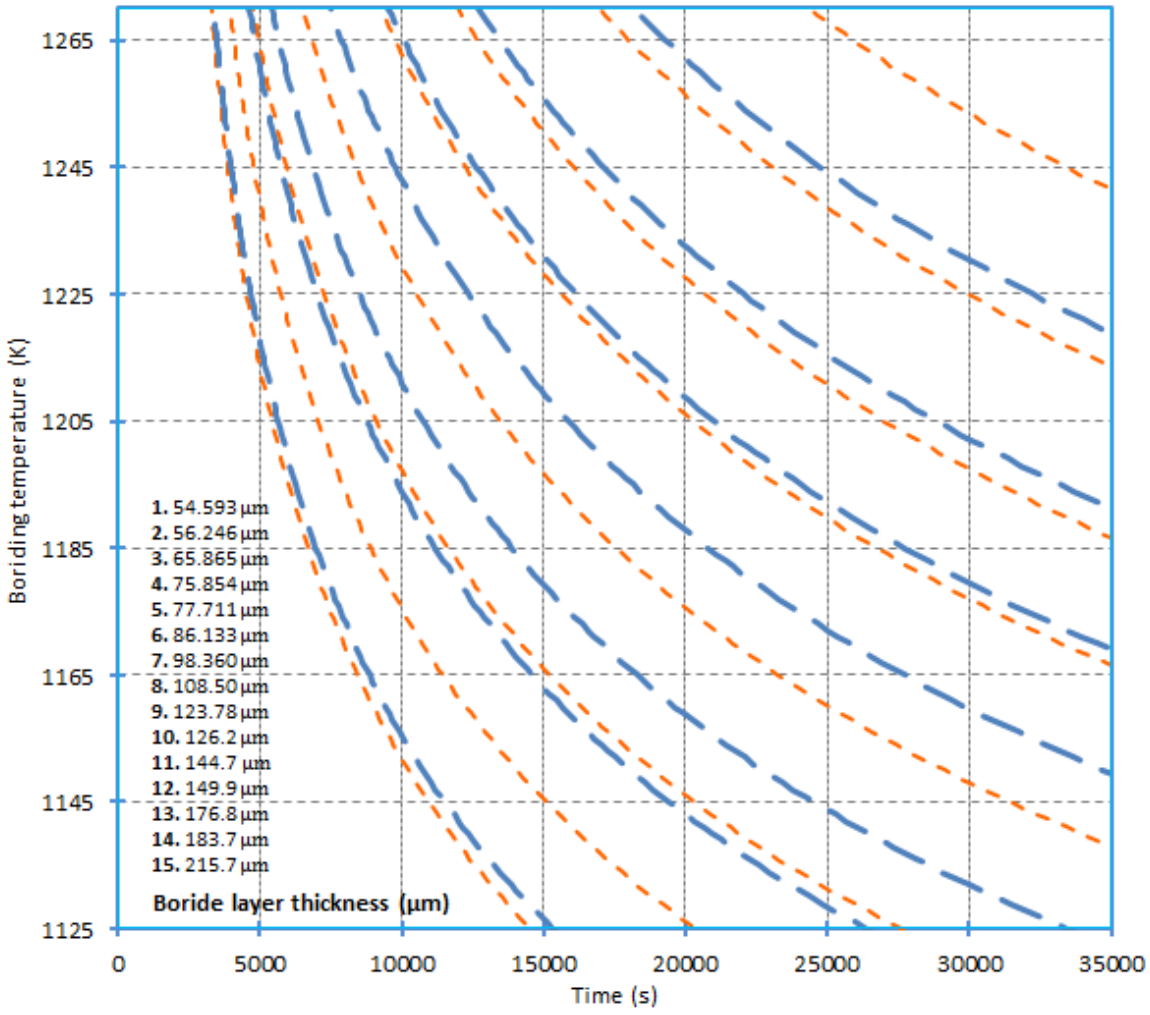

Figure 14. Iso-diagram describing the evolution of Fe_2B layer as a function of boriding parameters.

The results of **Figure 14** can serve as a powerful tool to select the optimum value of Fe_2B layer thickness in relation with the potential applications of the borided AISI 1026 in industrial scale.

As a rule, thin layers (e.g. 15–20 μm) are used to protect against adhesive wear (such as chipless shaping and metal stamping dies and tools), whereas thick layers are recommended to combat abrasive wear (extrusion tooling for plastics with abrasive fillers and pressing tools for the ceramic industry). In the case of low carbon steels and low alloy steels, the optimum boride layer thicknesses ranges from 50 to 250 μm, and for high- alloy steels, the optimum boride layer thicknesses ranges from 25 to 76 μm. Finally, this model can be extended to predict the growth kinetics of bilayer configuration ($FeB + Fe_2B$) grown on any boride steel.

4. Conclusions

The AISI 1026 steel was pack-borided in the temperature range of 1123-1273 K during a treatment time varying from 2 to 8 h. The Fe_2B layers were formed on the AISI 1026 steel substrate. A mathematical model was suggested to estimate the boron diffusion coefficient through the Fe_2B layers. The boron activation energy of the AISI 1026 steel was found to be equal to 178.43 kJ mol^1. This value was compared with the data reported in the literature.

The validity of the diffusion model was examined by comparing the experimental value of Fe_2B layer thickness obtained at a temperature of 1253 K for 7 h of treatment with that predicted by the model. In addition, interfacial adhesion of the Fe_2B layers (obtained at 1273 K for 4 h) on AISI 1026 steel substrate was investigated. As a result, it was found that the adhesion strength quality of this boride layer was related to HF3 category according to VDI 3198 norm.

Acknowledgements

The work described in this paper was supported by a grant of **CONACyT** and **PROMEP** México. Also, the authors want to thank to **Ing. Martín Ortiz Granillo**, who is in charge as *Director of the Escuela Superior de Ciudad Sahagún* which belongs to the Universidad Autónoma del Estado de Hidalgo, México, for all the facilities to accomplish this research work.

References

-Badini C. and Mazza D. (1988). *The texture of borided layers grown on Fe-Ni and Fe-Cr alloys.* Journal Materials Science Letters, (23): 661-665.

-Bindal C. and Ucisik AH. (1999). *Characterization of borides formed on impurity-controlled chromium-based low alloy steels.* Surface and Coatings Technology, (122): 208-213.

-Brakman C.M, Gommers A.W.J and Mittemeijer E.J. (1989). *Boriding Fe and Fe-C, Fe-Cr, and Fe-Ni alloys; Boride-layer growth kinetics.* J. Mater. Res. (4):1354-1370.

-Campos-Silva I, Oseguera J, Figueroa U, Garcian J.A, Bautista O and Keleminis G, (2003). Materials Science and Engineering- A, (352) : 261-265.

-Campos-Silva I, Bravo-Bárcenas D, Meneses-Amador A, Ortiz-Dominguez M, Cimenoglu H, Figueroa-López U and Tadeo-Rosas R. (2013). Surface and Coatings Technology, (237): 402-414.

-Campos-Silva I, Ortiz-Domínguez M, Bravo-Bárcenas O, Doñu-Ruiz M.A, Bravo-Bárcenas D, Tapia-Quintero C. and M.Y. Jiménez-Reyes. (2010). *Formation and kinetics of FeB/*Fe_2B *layers and diffusion zone at the surface of AISI 316 borided steels,* Surface and Coatings Technology, (205): 403-412.

-Celik O.N, Aydinbeyli N. and Gasan H. (2008). *Boride layer growth kinetics of the borided hypoeutectoid plain carbon steels by the powder-pack method.* Praktical Metallography, (45): 334-347.

-Dybkov V.I. (2010). *Reaction Diffusion and Solid State Chemical Kinetics*, Trans Tech Publications; 7.

-Gunes I, Ulker S, and Taktak S. (2013), *Kinetics of plasma paste boronized AISI 8620 steel in borax paste mixtures.* Protection of Metals and Physical Chemistry of Surfaces, (49): 567-573.

-Keddam M and Chegroune R, (2010), Applied Surface Science, (256): 5025-5030.

-Kulka M, Makuch N, Pertek A and Maldzinski L. (2013), *Simulation of the growth kinetics of boride layers formed on Fe during gas boriding in* H_2-BCl_3 *atmosphere*, Journal of Solid State Chemistry, (199):196-203.

-Meric C, Sahin S, and Yilmaz S.S, (2000), Mater. Res. Bull. (35): 2168.

-Okamoto H, (2004), Journal of Phase Equilibria and Diffusion, (25-3): 297-298.

-Ortiz-Domínguez M, (2013), *Contribución de la Modelación Matemática en el Tratamiento Termoquímico de Borurización.* PhD thesis. México: SEPI-ESIME from the Instituto Politécnico Nacional.

-Palombarini G and Carbucicchio M, (1987), *Growth of boride coatings on iron*, Journal of Materials Science Letter, (6): 415-416.

-Pertek A and Kulka M, (2002), Applied Surface Science, 252-260

-Rodríguez G, Campos-Silva I, Martínez-Trinidad J, Figueroa-López U, Meléndez-Morales D and Vargas-Hernández J, (2009), Adv. Mater. Res. (65): 63.

-Sinha A.K, (1991), Journal of Heat Treatment, (4): 437-447.

-Taktak S, (2007), *Some mechanical properties of borided AISI H13 and 304 steels.* Materials and Design, (28): 1836-1843.

-Taktak S, and Tasgetiren S, (2006), *Identification of Delamination Failure of Boride Layer on Common Cr-Based Steels*, Journal of Materials Engineering and Performance, (15-5): 570-573.

-Verein Deutscher Ingenieure Normen, (1991)- VDI 3198, Düsseldorf: VDI-Verlag; p. 1-8.

-Vidakis N, Antoniadis A, and Bilalis N, (2003), *The VDI 3198 indentation test evaluation of a reliable qualitative control of layered compounds*, Journal of Materials Process Technology, (143-144): 481-485.

-Vipin J, and Sundararajan G, (2002), *Influence of the pack thickness of the boronizing mixture on the boriding of steel*, Surface and Coatings Technology, (149): 21-26.

-Yu L.G, Chen X.J, Khor K.A, and Sundararajan G, (2005), *FeB/*Fe_2B *phase transformation during SPS pack-boriding*: Boride layer growth kinetics, Acta Materialia (53): 2361-2368.